nature medicine

SUPPLEMENTARY INFORMATION

https://doi.org/10.1038/s41591-018-0015-9

In the format provided by the authors and unedited.

MC4R agonism promotes durable weight loss in patients with leptin receptor deficiency

Karine Clément[1,12], Heike Biebermann[2,12], I. Sadaf Farooqi[3,12], Lex Van der Ploeg[4,12], Barbara Wolters[2], Christine Poitou[1], Lia Puder[2], Fred Fiedorek[4], Keith Gottesdiener[4], Gunnar Kleinau[5], Nicolas Heyder[5], Patrick Scheerer[5,6], Ulrike Blume-Peytavi[7], Irina Jahnke[7], Shubh Sharma[4], Jacek Mokrosinski[3], Susanna Wiegand[8], Anne Müller[2], Katja Weiß[9], Knut Mai[6,10], Joachim Spranger[6,10], Annette Grüters[11], Oliver Blankenstein[2], Heiko Krude[2] and Peter Kühnen[2]*

[1]Sorbonne Université, INSERM, NutriOmics team, Assistance Publique-Hôpitaux de Paris, Pitié-Salpêtrière Hospital, Paris, France. [2]Institute for Experimental Pediatric Endocrinology, Charité – Universitätsmedizin Berlin, corporate member of Freie Universität Berlin, Humboldt-Universität zu Berlin and Berlin Institute of Health, Berlin, Germany. [3]University of Cambridge Metabolic Research Laboratories and NIHR Cambridge Biomedical Research Centre, Wellcome Trust-MRC Institute of Metabolic Science, Addenbrooke's Hospital, Cambridge, UK. [4]Rhythm Pharmaceuticals, Boston, MA, USA. [5]Institute of Medical Physics and Biophysics, Group Protein X-ray Crystallography and Signal Transduction, Charité – Universitätsmedizin Berlin, corporate member of Freie Universität Berlin, Humboldt-Universität zu Berlin and Berlin Institute of Health, Berlin, Germany. [6]DZHK (German Centre for Cardiovascular Research), partner site Berlin, Berlin, Germany. [7]Department of Dermatology and Allergy, Clinical Research Center for Hair and Skin Science, Charité – Universitätsmedizin Berlin, corporate member of Freie Universität Berlin, Humboldt-Universität zu Berlin and Berlin Institute of Health, Berlin, Germany. [8]Center for Chronic Sick Children, Charité – Universitätsmedizin Berlin, corporate member of Freie Universität Berlin, Humboldt-Universität zu Berlin and Berlin Institute of Health, Berlin, Germany. [9]Department of Pediatric Cardiology, Charité – Universitätsmedizin Berlin, corporate member of Freie Universität Berlin, Humboldt-Universität zu Berlin and Berlin Institute of Health, Berlin, Germany. [10]Department of Endocrinology, Diabetes, and Nutrition and Charité Center for Cardiovascular Research, Charité – Universitätsmedizin Berlin, corporate member of Freie Universität Berlin, Humboldt-Universität zu Berlin and Berlin Institute of Health, Berlin, Germany. [11]Department of Pediatric Endocrinology and Diabetes, Charité – Universitätsmedizin Berlin, corporate member of Freie Universität Berlin, Humboldt-Universität zu Berlin and Berlin Institute of Health, Berlin, Germany. 12These authors contributed equally: Karine Clément, Heike Biebermann, I. Sadaf Farooqi, Lex Van der Ploeg. *e-mail: peter.kuehnen@charite.de

Supplementary information

Supplemental results and discussion:

Our human (h) MC4R/alpha-MSH and hMC4R/setmelanotide complex models suggest that the peptidic agonists bind generally into a cleft between the extracellular loops (E1-3) and the transmembrane helices (TMHs or Hs) (**supplementary Figures 7 and 8**). Approximately twenty hMC4R amino acids are constituting the ligand binding pockets. Specific parts of the N-terminus are also supposed to participate in alpha-MSH binding, *e.g.* by interactions of Lys33 or Asp37. However, these residues are not conserved among members of the MCR (melanocortin receptor) group, which may exclude a significant role for alpha-MSH binding.

Analyzing the docking complexes specific emphasis relays on the interactions and localization of the conserved ligand motif HFRW. For alpha-MSH this central amino acid motif ($_6$HFRW$_9$) is known to be involved in ligand recognition and induction of ligand effects[24] and here supposed main interactions with the receptor are (*alpha-MSH*/MC4R): *Trp9*/Phe261; *Arg8*/Glu100, Asp126, Asp122; *Phe*7/Phe184; and *His6*/Tyr268. Most of these interactions are also supposed for setmelanotide, e.g. the Arg6 (corresponds with Arg8 in alpha-MSH) interact with negatively charged side chains of MC4R Glu100, Asp122 and Asp126. Moreover, Trp9 in alpha-MSH and corresponding Trp7 in setmelanotide are both embedded by aromatic interactions with Phe261 in H6 and Phe284 in H7, in close proximity also to a MC4R activation related residues[25,26] Tyr268 (H6) and His283 in the H7-E3 transition.

Despite partial overlap in the MC4R/alpha-MSH and MC4R/setmelanotide interaction pattern also differences can be observed, which might be reasoned by the fact that setmelanotide is a cyclic peptide with a disulfide bridge between two cysteines and in consequence is more rigid in the backbone compared to MSH. Specifically the ligand histidines in the ligand HFRW motifs are oriented differently in both docking poses. The histidine in setmelanotide is located between Asn123 (H3) and Phe184 (H4), but in the alpha-MSH/MC4R complex the corresponding His6 is directed between Tyr268 and Ser191 of the receptor. Moreover, alpha-MSH Phe7 interacts with Cys130 in H3 and Phe184 in H4, whereby the corresponding Phe5 of setmelanotide is oriented towards H6 and interacts additionally with Phe261. Therefore, it can be postulated that despite shared interactions of both ligands with MC4R these differences in detailed interactions contribute to the diverse pharmacological profiles (**supplementary Figure 10**).

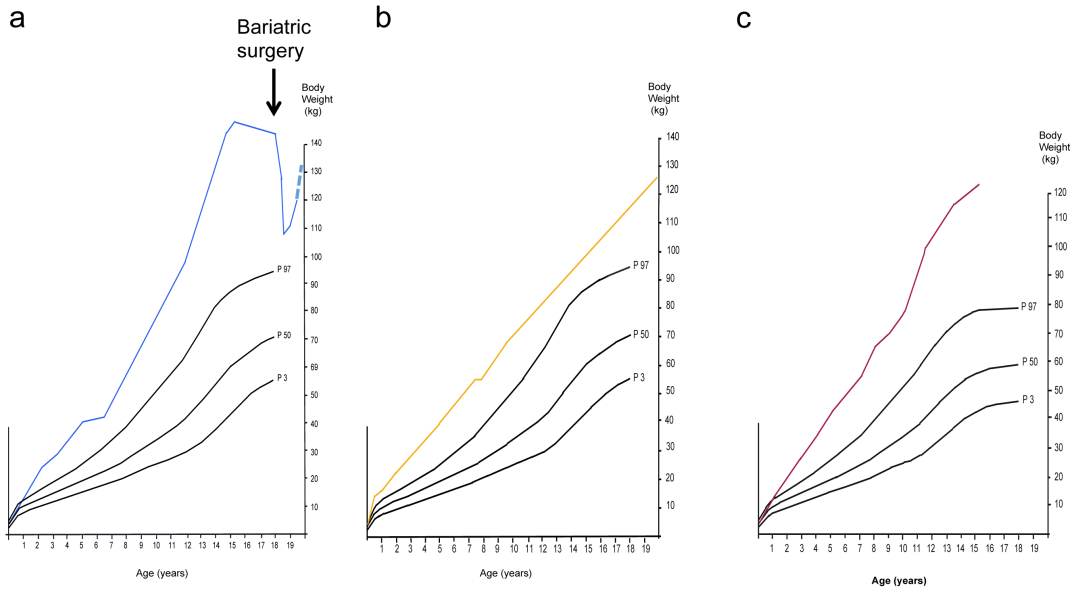

Supplementary Figure 1 Weight course of LEPR patients before setmelanotide treatment start.

Weight course of the three included subjects with LEPR deficiency **(a-c)** before the study start. Standard percentiles were used[27]. All of them had a history of early onset obesity and severe hunger and were not able – despite tremendous effort - to stabilize the body weight over a longer period of time. Subject 1 with LEPR deficiency **(a)** had a gastric banding operation, which led to a short interval of weight loss and subsequent weight regain. The dashed blue line visualized the weight gain months before the treatment start and is not adapted to the time scale of the y-axis. Additionally for subject 2 weight data are not available between 8 and 19 years of age.

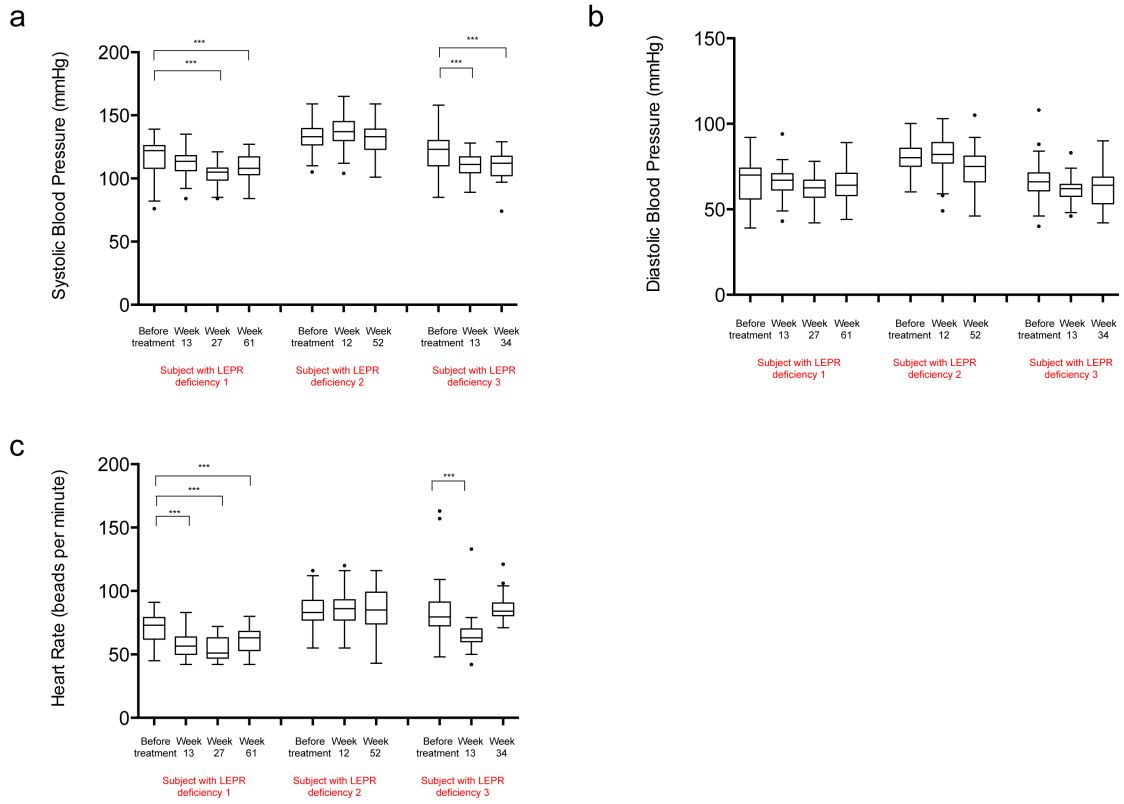

Supplementary Figure 2 Blood pressure and heart rate before and during setmelanotide treatment.

24-hours ambulatory blood pressure monitoring before and during treatment with setmelanotide in three enrolled individuals with LEPR deficiency **(a-c)**. Statistical analysis was performed using one-sided t-test analyzing “before treatment” data against each outlined week of treatment separately (*** = $p < 0.001$). Subject 1: before treatment n=67 individual measurements, week 13 n=68 individual measurements, week 27 n=54 individual measurements, week 61 n=51 individual measurements; subject 2: before treatment n=57 individual measurements, week 12 n=59 individual measurements, week 52 n=87 individual measurements; subject 3: before treatment n=54 individual measurements, week 13 n=33 individual measurements, week 34 n=22 individual measurements. In the box plots horizontal line inside each box indicates median and the top and bottom of the box indicate the interquartile range. The bars indicate the 5th and 95th percentiles and dots indicate outliers.

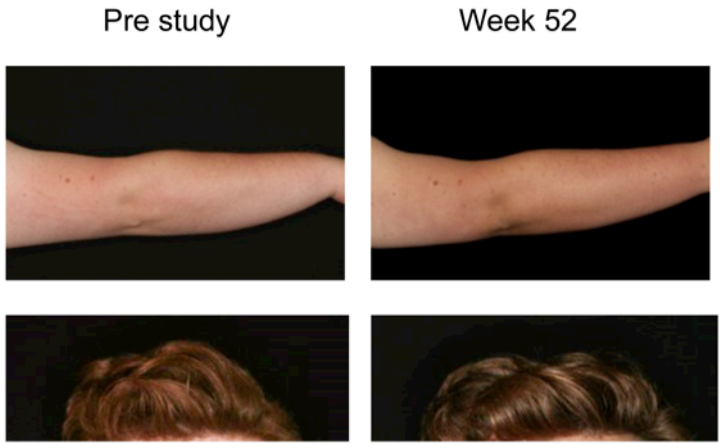

Supplementary Figure 3 Skin and hair color.
Examples of changes in skin color during the MC4R agonist treatment before and after 52 treatment weeks in individual 2 with LEPR deficiency. Additionally, in subject 2 with LEPR deficiency the treatment led additionally to a change of the hair color from red to brown.

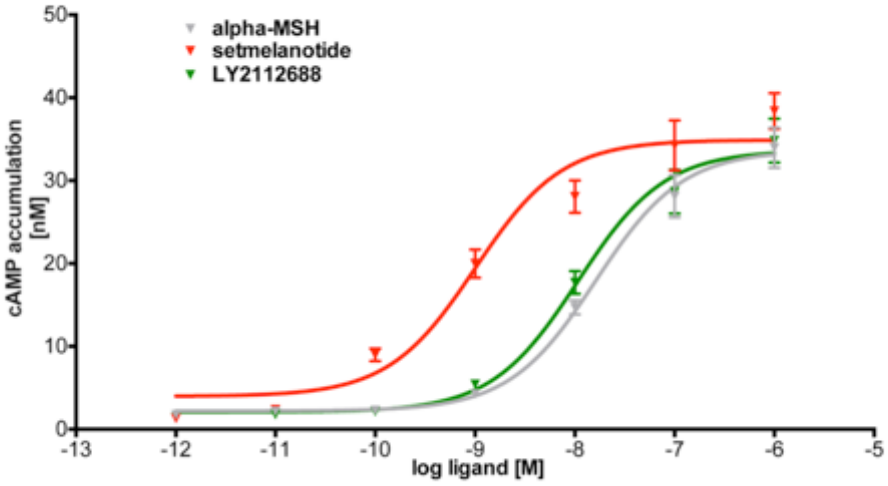

Supplementary Figure 4 Determination of setmelanotide, alpha-MSH and first generation MSH LY2112688 induced effect on cAMP formation.
HEK293 cells were transiently transfected with MC4R and stimulated with indicated ligand concentrations. Results of seven independent experiments performed in triplicated were shown as raw data, data are mean ± s.e.m.. Statistical analysis was performed using a one-way ANOVA with Kruskal-Wallis test at a concentration of 10^{-8} M. Setmelanotide was tested against alpha-MSH and LY2112688: **** for alpha-MSH, and ** for LY2112688, ** $p \leq 0.01$, **** $p \leq 0.0001$.

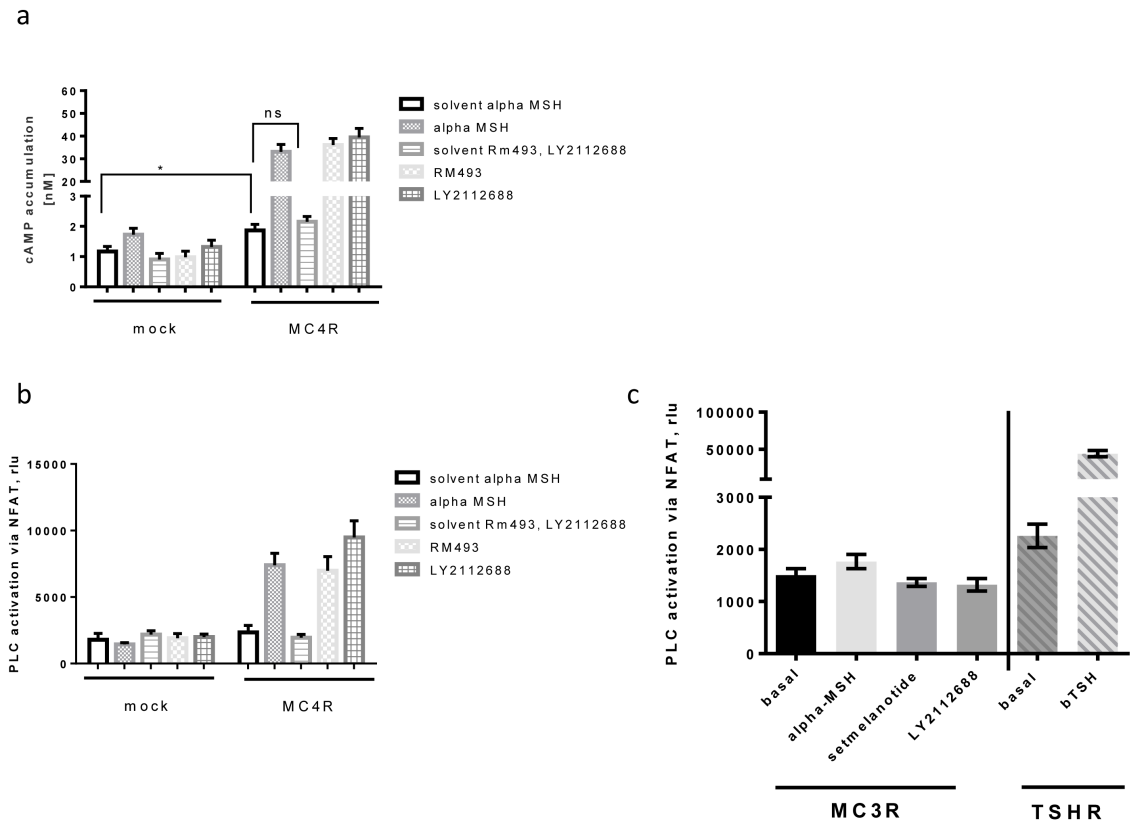

Supplementary Figure 5 Controls for off-target effect of solvents for alpha-MSH, setmelanotide and LY2112688 and effects at MC3R.
HEK293 cells were transfected with empty vector (mock) and MC4R **(a, b)** or MC3R and TSHR **(c)**. The result of four independent experiments performed in triplicates is shown as raw data, data represents mean ± s.e.m.. **(a)** mock transfected cells were stimulated with the solvent for alpha-MSH (PBS with 0.001% BSA) and the solvent for setmelanotide and LY2112688 (PBS with 0.1% DMSO). Statistical analysis was performed using a one-way ANOVA with Kruskal-Wallis test and reveled no statistical difference. MC4R transfected cells were stimulated with alpha-MSH (1 µM) and the solvent for ligands. Basal activity of MC4R tested against mock transfection by unpaired t-test with Welsh correction and solvent effects at MC4R were tested against MC4R under basal condition by one-way ANOVA with Kruskal-Wallis test and revealed no statistical significance. **(b)** Identical set of experiments and statistical tests for activation for PLC as is indicated in **(a)**. **(c)** *HEK293* cells were co-transfected with MC3R or TSHR and a reporter gene for NFAT and PLC activation was tested. TSHR was stimulated with 100 mU/ml bTSH and served as control. MC3R was stimulated with indicated ligands (1 µM). Statistical significance was tested by one-way ANOVA with Kruskal-Wallis test and revealed no difference.

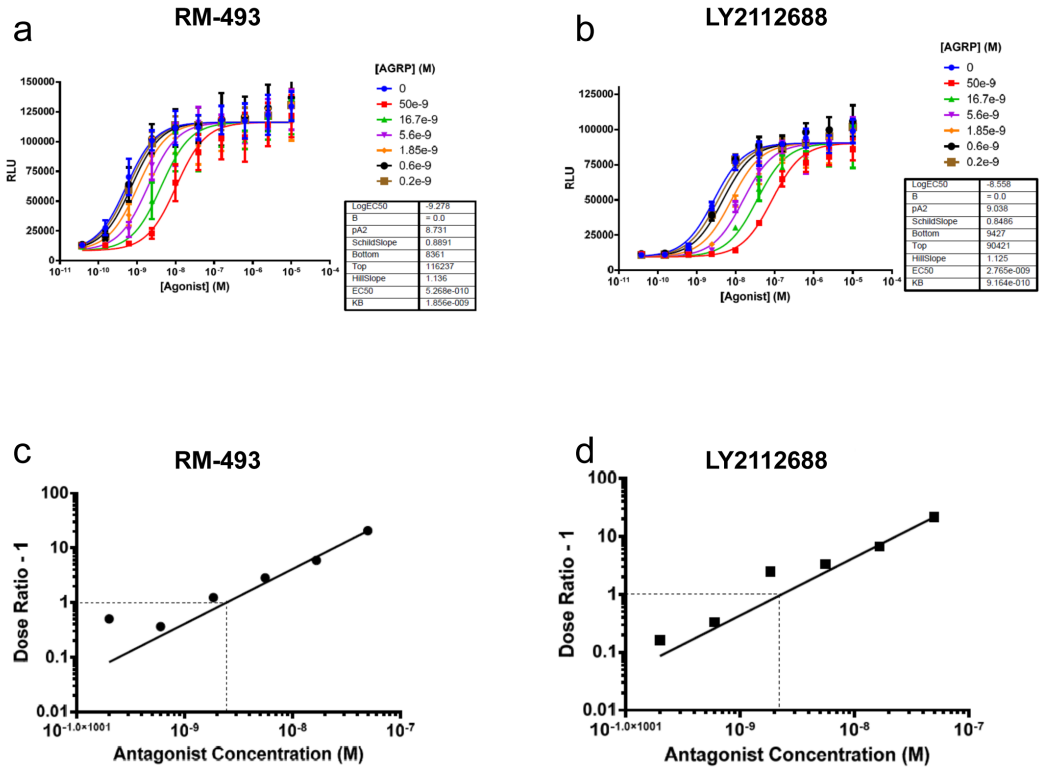

Supplementary Figure 6 Setmelanotide and LY2112688 activated cAMP signaling after AgRP stimulation.
(**a-d**): Complete cAMP stimulation concentration response for the agonist was performed both in the absence and in the presence of six concentrations of the AgRP (ranging from 0.2nM to 50nM). Each concentration response curve for the agonist used 10 concentrations (ranging from 0.38pM to 10μM), which were challenged with one of the six concentrations of AgRP. The data was analyzed by non-linear regression analysis, and Schild's analysis using DR-1 versus antagonist concentration (**c-d**). The result of one representative experiment performed in triplicates is shown and data are given as mean ± s.e.m..
The comparative EC50 for setmelanotide (**a, c**) and LY2112688 (**b, d**) for cAMP stimulation were given.

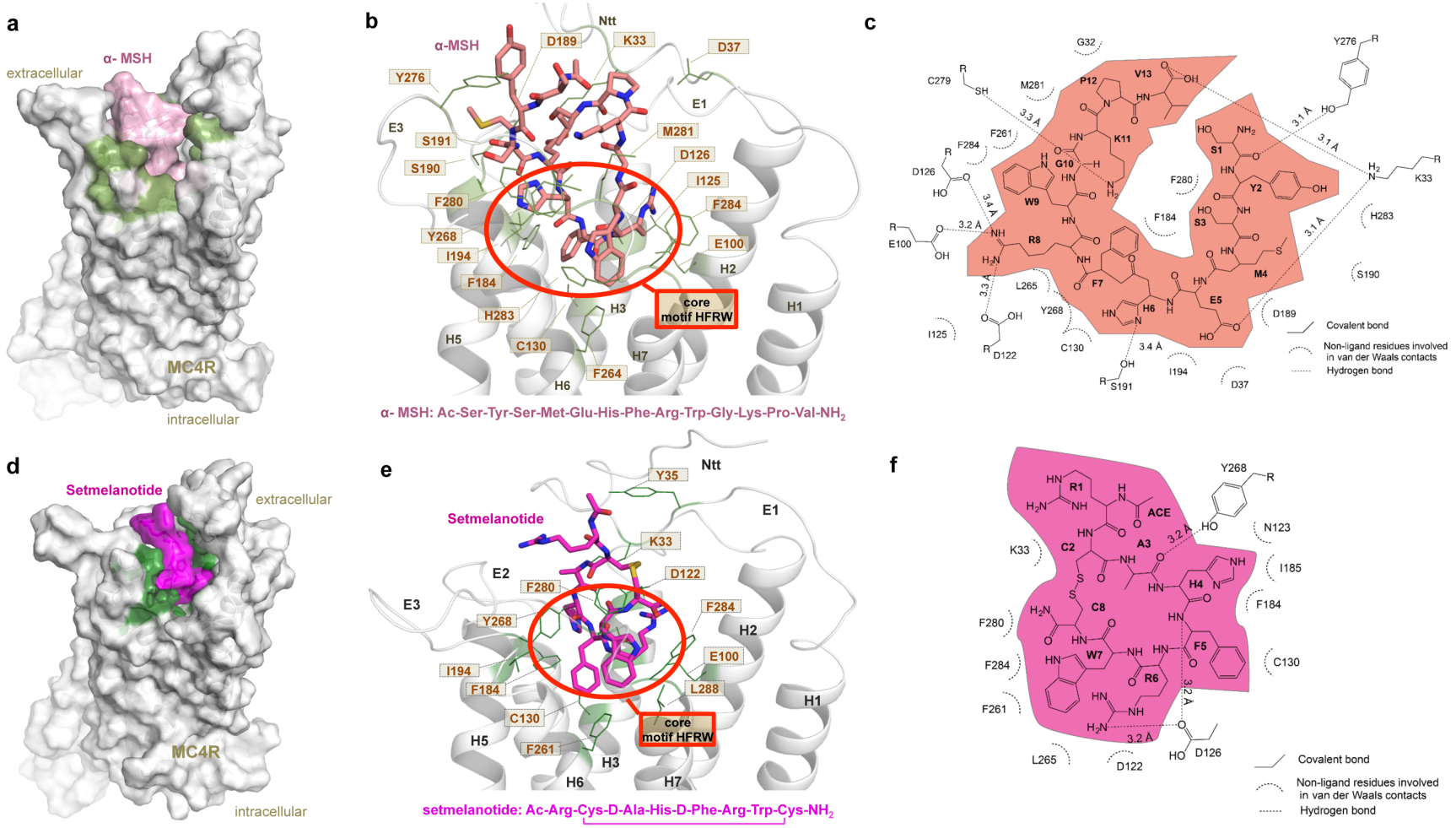

Supplementary Figure 7 Structural models of MC4R-ligand complexes.
(a) The human hMC4R/alpha-MSH complex model (in surface representation) reveals that the peptidic agonist binds into a cleft between the extracellular loops (E1-3) and specific transmembrane helices (H). Amino acids covering the ligand binding pocket are

colored pale-green. **(b)** Approximately twenty hMC4R amino acids (green lines) in the transmembrane region and in the E2 or E3 constituting the ligand binding pocket. Importantly, in alpha-MSH (amino acid sequence of alpha-MSH below the model-figure) a central amino acid motif $_6$HFRW$_9$ is involved in ligand recognition and induction of ligand effects[24]. This specific ligand motif is located between the helices and their extracellular ends. **(c)** The detailed interaction map for the MC4R/alpha-MSH complex shows a schematic overview of supposed interactions. (**d**) The surface representation of the MC4R/setmelanotide complex model highlights the general localization of this ligand bound to the hMC4R. Amino acids covering the supposed setmelanotide binding pocket are colored green. **(e)** The cyclic peptide agonist setmelanotide (amino acid sequence below the model-figure) interacts, comparable to alpha-MSH, with the MC4R by a supposed salt bridge between the ligand Arg6 in the central core and the negatively charged receptor residues Glu100 (TMH2), Asp122 and Asp126 (TMH3) in MC4R. **(f)** The interaction map between setmelanotide and MC4R shows a different interaction pattern as supposed for alpha-MSH at MC4R, however, there is partial overlap in participating MC4R amino acids such as Asp122, Glu100 or Phe284. Potential hydrogen bonds were analyzed using HBPLUS[28] as implemented in the program LIGPLOT$^+$1.45[29]. Residues with distances less than 3.9 Å were considered to be in van der Waals contact.

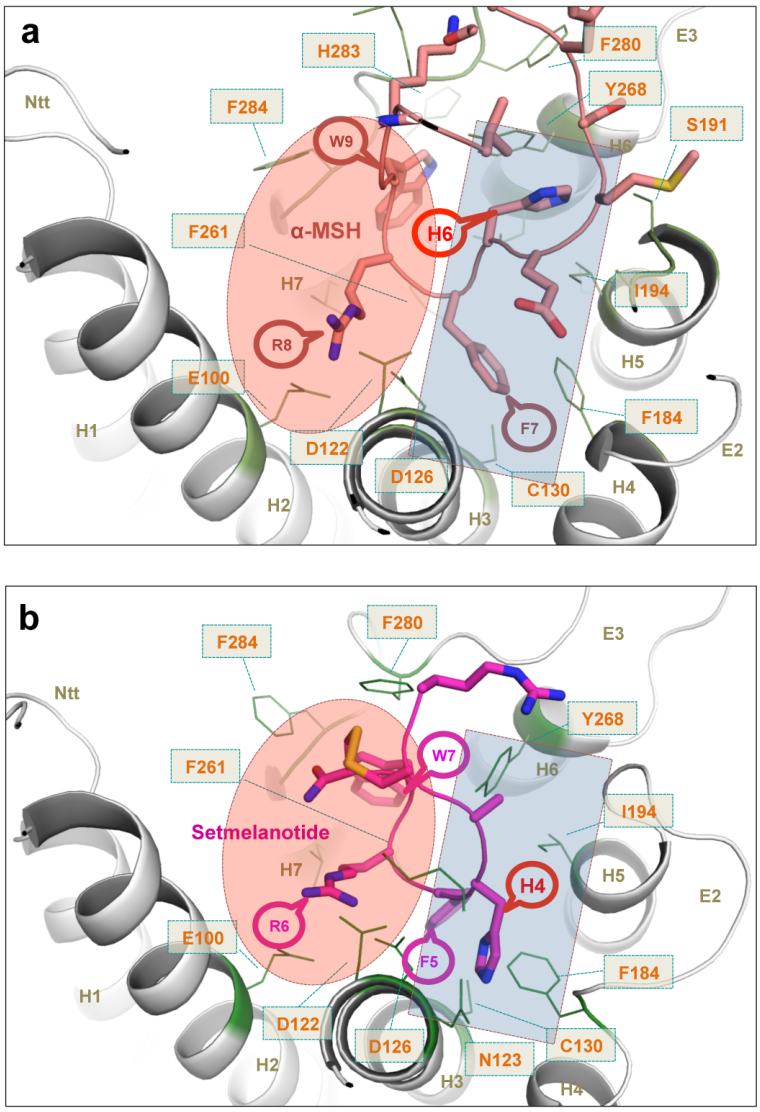

Supplementary Figure 8 Comparison between binding modes of setmelanotide and alpha-MSH at hMC4R.

The putative binding modes of (**a**) alpha-MSH and (**b**) setmelanotide at hMC4R reveal similarities and differences between both ligands (shown as Cα-backbone cartoon representation and clipped models). Of note, in contrast to α-MSH, setmelanotide is a cyclic peptide with a disulfide bridge between two cysteines. A specific emphasis relays on the interactions and localization of the conserved ligand motif HFRW. The Arg6 (setmelanotide) and Arg8 (alpha-MSH) interact with negatively-charged side chains of Glu100 (TMH2) and Asp122/Asp126 in H3 of the receptor. Moreover, Trp9 in alpha-MSH and corresponding Trp7 in setmelanotide are both embedded by aromatic interactions with Phe261 in H6 and Phe284 in H7, in close proximity also to a activation related receptor residues[25,26] Tyr268 in H6 and His283 in the H7-E3 transition. In the MC4R/ setmelanotide complex additionally Phe280 participates in the interaction with Trp7. However, specifically the histidine (shown with red label) of the ligands is oriented differently in both docking poses. The histidine in setmelanotide is located between Asn123 (H3) and Phe184 (H4), but in the alpha-MSH/MC4R complex the corresponding His6 is directed between Tyr268 and Ser191 of the receptor. Moreover, alpha-MSH Phe7 interacts with Cys130 in H3

and Phe184 in H4, whereby the corresponding Phe5 of setmelanotide is oriented towards H6 and interacts additionally with Phe261. It can be concluded that *(i)* both ligands potentially share specific interactions of the highly conserved motif HFRW with MC4R (shown as red filled translucent circle), on the other hand *(ii)* the corresponding ligand histidines and phenylalanines in this motif are different in detailed interactions with side chains in receptor helices 4-6 (shown as blue filled translucent rectangle).

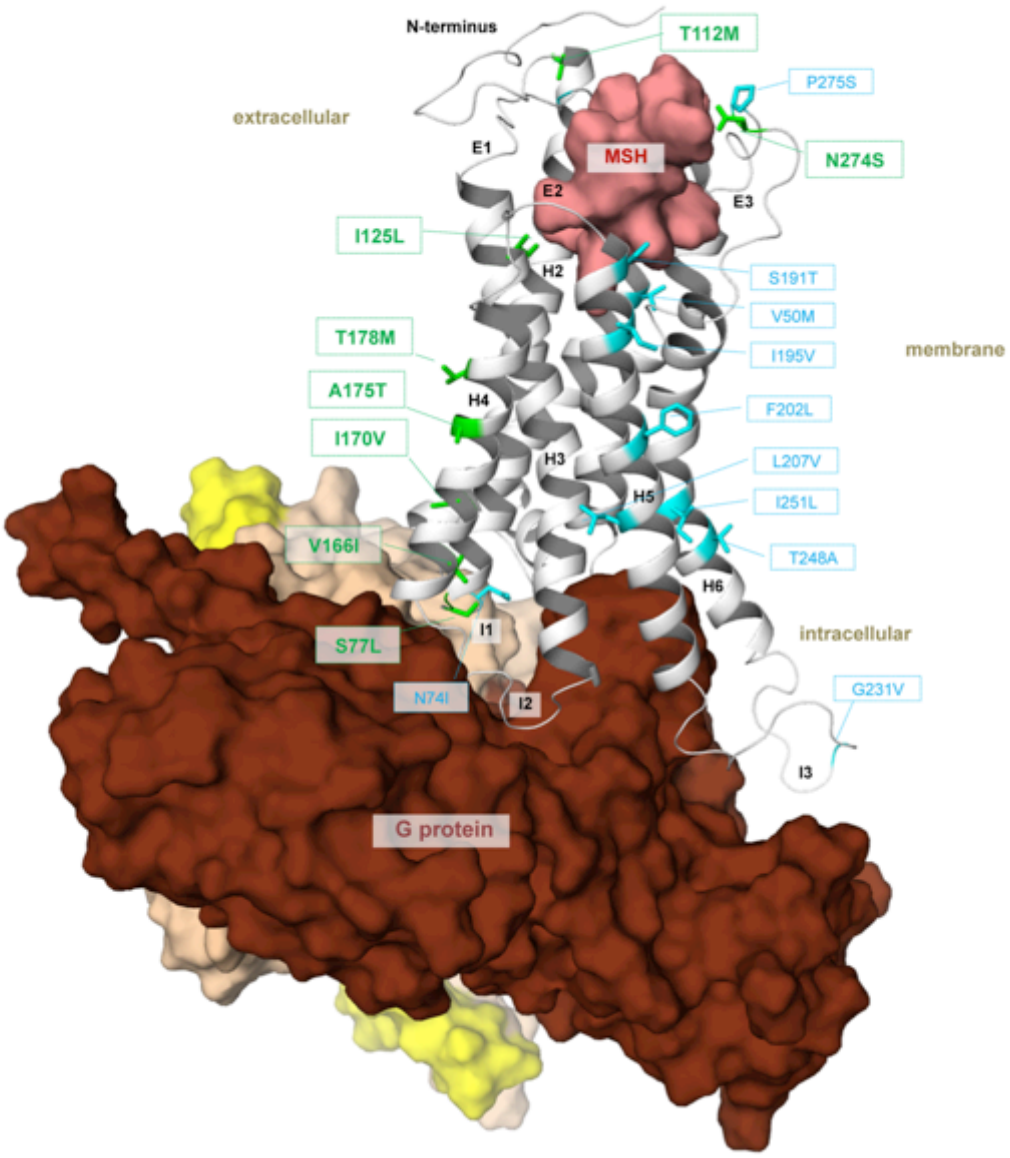

Supplementary Figure 9 Structural homology model of alpha-MSH/hMC4R/G-protein complex with highlighted positions of mutants reported to be “like wild-type” for Gαs mediated signaling.
Wild-type amino acids (green sticks) of in this study experimentally tested *MC4R* mutants concerning their $G\alpha_q$ and Gαs signaling properties **supplementary Table 5**) are highlighted at a MC4R/ligand complex model extended by a heterotrimeric G-protein molecule (surface representation, α-subunit in brown, β-subunit in light-brown, γ-subunit in yellow). These positions are located in helices (H) H2, H3 and are cumulated in H4. Moreover, we also exemplarily show further wild-type residues (cyan sticks) which were reported to be identified in obese patients and characterized *in vitro* as “like wild-type” mutations for cAMP accumulation. Of note, from the around 160 reported naturally occurring hMC4R single side chain variants approximately 30% were characterized so far “like wild-type” in Gαs mediated signaling.

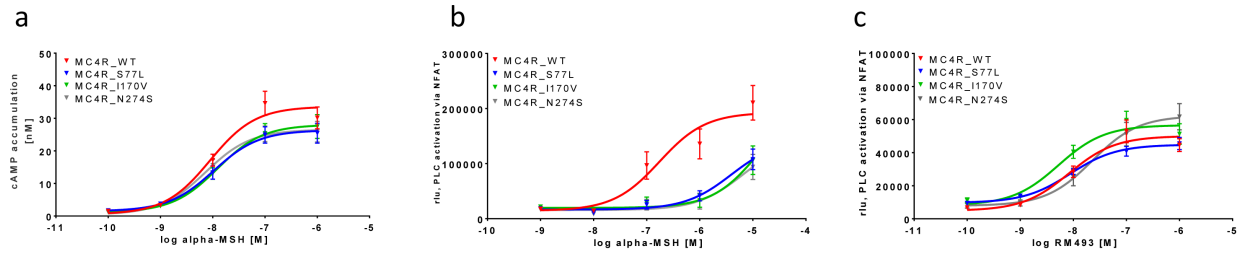

Supplementary Figure 10 Functional characterization of like wild-type *MC4R* variants in Gαs and PLC signaling after alpha-MSH and setmelanotide challenge. *HEK293* cells were transfected with MC4R wild-type and indicated *MC4R* variants and stimulated with indicated ligand concentrations. **(a)** cAMP accumulation after stimulation with alpha-MSH. **(b, c)** All *MC4R* mutants were tested for PLC signaling after co-transfection with NFAT reporter gene. Stimulation was performed with alpha-MSH **(b)** and setmelanotide **(c)**. Raw data of four independent experiments are shown, data are mean ± s.e.m..

Supplement Table 1

Laboratory values subject with LEPR deficiency 1:

	Pre-study	After 13 weeks	After 27 weeks	After 61 weeks	Reference value
Cholesterol (mg/dl)	168	135	138	127	<200
HDL (mg/dl)	52	46	55	62	>45
LDL (mg/dl)	102	78	76	63	<130
Triglyceride (mg/dl)	57	53	40	36	<200
ALT (U/l)	20	19	10	28	<41
AP (U/l)	62	64	67	60	40-130
gamma-GT (U/l)	21	13	10	17	8-61
Cortisol (nmol/l)	199.8	319.4	243.2	287.0	
Testosterone (µg/l)	4.64	2.38	6.81	5.53	2.18-9.06
fT4 (ng/l)	12.48	11.7	10.64	13.04	9.3-17
TSH (mU/l)	0.59	0.99	0.88	0.52	0.27-4.2
HbA1c (%)	5.1	5.1	5.2	5.2	<6.0

Oral glucose tolerance test subject with LEPR deficiency 1:

	Pre-study		After 13 weeks		After 27 weeks		After 61 weeks	
Time point (min)	Blood glucose (mg/dl)	Insulin (mU/l)	Blood glucose (mg/dl)	Insulin (mU/l)	Blood glucose (mg/dl)	Insulin (mU/l)	Blood glucose (mg/dl)	Insulin (mU/l)
0	75	6.09	76	69.74	73	3.72	71	1.89
30	164	119.8	108	58.03	131	9.23	113	39.80
60	147	89.92	152	92.55	74	56.24	161	106.00
90	130	67.02	128	66.44	64	30.25	136	65.10
120	114	46.02	117	64.44	101	42.94	104	29.40

Supplementary Table 1 Laboratory parameters subject 1.
Laboratory safety parameter and oral glucose tolerance test results of subject 1 with LEPR deficiency.

Supplement Table 2

Laboratory values subject with LEPR deficiency 2:

	Pre-study	After 12 weeks	After 52 weeks	Reference value
Cholesterol (mg/dl)	173	186	184	<200
HDL (mg/dl)	34	44	49	>45
LDL (mg/dl)	122	138	124	<130
Triglyceride (mg/dl)	141	123	103	<200
AP (U/l)	74	80	64	40-130
Cortisol (nmol/l)	184.8	364.4	216	
Testosterone (µg/l)	2.11	3.78	2.82	2.18-9.06
fT4 (ng/l)	11.49	10.55	9.73	9.3-17
TSH (mU/l)	1.27	2.43	1.85	0.27-4.2
HbA1c (%)	5.3	5.0	5.3	<6.0

Oral glucose tolerance test subject with LEPR deficiency 2:

	Pre-study		After 12 weeks		After 52 weeks	
Time point (min)	Blood glucose (mg/dl)	Insulin (mU/l)	Blood glucose (mg/dl)	Insulin (mU/l)	Blood glucose (mg/dl)	Insulin (mU/l)
0	74	15.25	77	17.29	73	9.12
30	131	128.5	109	95.59	152	11.23
60	153	126.8	121	75.20	137	69.40
90	136	115.4	161	102.20	126	100.40
120	129	131.2	145	93.11	114	107.40

Supplementary Table 2 Laboratory parameters subject 2.
Laboratory safety parameter and oral glucose tolerance test results of subject 2 with LEPR deficiency.

Supplement Table 3

Laboratory values subject with LEPR deficiency 3:

	Pre-study	After 13 weeks	After 34 weeks	Reference values
Cholesterol (mg/dl)	150	134	151	92-234
HDL (mg/dl)	34	34	43	>45
LDL (mg/dl)	99	92	102	<130
Triglyceride (mg/dl)	92	82	46	<200
AP (U/l)	24	na	67	<187
Cortisol (nmol/l)	206	175.1	266	48.0-579.0
Prolactin (µg/l)	8.38	6.06	9.27	4.2-29.01
T4 (µg/l)	79.5	75.8	81.7	59.1-132.0
fT4 (ng/l)	12.2	13.04	13.21	8.90-14.90
TSH (mU/l)	1.45	0.63	1.14	0.60-4.00
HbA1c (%)	5.3	5.0	5.4	<6.0

Oral glucose tolerance test subject with LEPR deficiency 3:

	Pre-study		After 13 weeks		After 34 weeks	
Time point (min)	Blood glucose (mg/dl)	Insulin (mU/l)	Blood glucose (mg/dl)	Insulin (mU/l)	Blood glucose (mg/dl)	Insulin (mU/l)
0	86	395.7	69	5.86	83	32.90
30	161	231.3	99	127.90	132	220.00
60	140	296.2	144	162.30	146	281.00
90	129	na	149	260.80	103	284.00
120	137	378.0	94	54.85	112	230.00

Supplementary Table 3 Laboratory parameters subject 3.
Laboratory safety parameter and oral glucose tolerance test results of subject 3 with LEPR deficiency.

AE description	Number of patients in which AE occurred	Severity	Duration (days; listed for each patient)
Reduced appetite	3	severe	ongoing
Increased tanning of the skin/ nevi	3	severe	ongoing
Skin folliculitis	1	mild	ongoing
Pain at injection site	2	mild	3 / 8
Induration/ hematoma at injection site	2	mild	2 / 2
Bone & muscular pain	2	mild	2 / 4
Dry mouth	3	mild	2 / 7 / ongoing
Headache	3	mild	1 / 2 / 7
Nausea	1	mild	2
Abdominal pain	1	mild	1
SAE description			
none			

Supplementary Table 4 Summary of adverse events
Adverse events (AEs), which have occurred during the treatment duration of the subjects with LEPR deficiency, are listed with information about frequency, severity and duration. In cases where more than one subject reported an AE, the duration for each individual is listed in days. The total duration of treatment reported in this AE table is ~574 days for subject 1, ~483 days for subject 2, and ~343 days for subject 3.

	Gs/cAMP accumulation					PLC/NFAT activation				
		alpha-MSH		setmelanotide			alpha-MSH		setmelanotide	
mutation	basal signaling [fold over wild-type basal]	Emax at 10^{-6}M [fold over wild-type basal]	EC50 [nM]	Emax at 10^{-6}M [fold over wild-type basal]	EC50 [nM]	basal signaling [fold over wild-type basal]	Emax at 10^{-6}M [fold over wild-type basal]	EC50 [nM]	Emax at 10^{-6}M [fold over wild-type basal]	EC50 [nM]
wild-type	1	13.1 ± 1.3	8.4 ± 1.9	24 ± 4.0	7.1 ± 2	1	7.14 ± 2.11	174	6.9 ± 0.13	9.5 ± 1.4
T11I	0.83 ±0.05	12.3 ± 1.5	8.5 ± 0.9	19 ± 1.3	8.7 ± 2.8	0.92 ± 0.09	6.24 ± 1.15	806	6.0 ± 0.57	12 ± 3.4
S77L	0.99 ± 0.03	11.2 ± 1.1	10 ± 2.7	16 ± 0.5	3.4 ± 0.2	1.27 ± 0.15	2.3 ± 0.52	n.d.	6.3 ± 1.13	8.8 ± 0.4
T112M	0.72 ± 0.04[b]	10.6 ± 0.8	8.3 ± 1.6	18 ± 1.5	43 ± 15	1.4 ± 0.11	3.29 ± 0.55	n.d.	11.3 ± 2.9	14 ± 6
V166I	0.79 ± 0.08[a]	9.0 ± 2.2	20 ± 6.7	5.9 ±1.5	9.6 ± 3.2	1.81 ± 0.18[a]	0.33 ± 0.08[b]	n.d.	3.3 ± 0.79	n.d.
I170V	0.87 ± 0.06	11.1 ± 2.7	17 ± 4.3	11 ± 2.7	37 ± 9.2	1.22 ± 0.13	1.89 ± 0.4	n.d.	7.3 ± 1.8	5.2 ± 1.3
A175T	0.78 ± 0.07	12.5 ± 3.1	13 ± 3.1	17 ± 4.4	15 ± 5.1	0.87 ± 0.17	2.87 ± 0.71	n.d.	11.7 ± 2.9	26 ± 6.6
T178M	0.96 ± 0.12	13.2 ± 4.3	10 ± 3.3	21 ± 5.2	68 ± 17	1.10 ± 0.21	2.87 ± 0.71	n.d.	9.2 ± 2.3	24 ± 6
I251L	0.76 ± 0.09[b]	10.4 ± 2.6	11 ± 2.7	18 ± 4.5	4.8 ± 1.2	0.92 ± 0.14	4.46 ± 1.15	n.d.	7.5 ± 1.9	18 ± 4.3
N274S	0.8 ± 0.1[a]	11.4 ± 2.8	7.6 ± 1.9	14 ± 3.4	43 ± 11	1.29 ± 0.22	1.65 ± 0.41	n.d.	8.4 ± 2.1	12 ± 4

Supplementary Table 5 Functional characterization of “like wild-type” *MC4R* variants.

MC4R variants that were classified as “like wild-type” concerning Gαs/adenylyl cyclase signaling were evaluated for their capacity to induce NFAT signaling after alpha-MSH and setmelanotide challenge. *HEK293* cells were transfected with indicated variants for determination of cAMP accumulation and co-transfected with NFAT reporter in case of PLC determination. Given data are results of four independent experiments performed in triplicates and are shown as mean ± s.e.m.. Comparison of variant-MC4R to wild-type MC4R stimulated with the same ligand was performed: a: * $p < 0.05$, b: ** $p < 0.01$ analyzed by one-way ANOVA with Kruskal-Wallis test. n.d.: not possible to determine with proper accuracy.

Supplemental references:

24. Ericson, M.D., *et al.* Bench-top to clinical therapies: A review of melanocortin ligands from 1954 to 2016. *Biochim Biophys Acta* **1863**, 2414-2435 (2017).
25. Tao, Y.X. The melanocortin-4 receptor: physiology, pharmacology, and pathophysiology. *Endocr Rev* **31**, 506-543 (2010).
26. Hogan, K., *et al.* Mapping the binding site of melanocortin 4 receptor agonists: a hydrophobic pocket formed by I3.28(125), I3.32(129), and I7.42(291) is critical for receptor activation. *J Med Chem* **49**, 911-922 (2006).
27. Kromeyer-Hauschild, M.W., D. Kunze, F. Geller, H.C. Geiß, V. Hesse, A. von Hippel, U. Jaeger, D. Johnsen, W. Korte, K. Menner, G. Müller, J.M. Müller, A. Niemann- Pilatus, T. Remer, F. Schaefer, H.-U. Wittchen, S. Zabransky, K. Zellner, A. Ziegler, J. Hebebrand. Perzentile für den Body-mass-Index für das Kindes- und Jugendalter unter Heranziehung verschiedener deutscher Stichproben. *Monatszeitschrift Kinderheilkude* **149**, 807-818 (2001).
28. McDonald, I.K. & Thornton, J.M. Satisfying hydrogen bonding potential in proteins. *J Mol Biol* **238**, 777-793 (1994).
29. Laskowski, R.A. & Swindells, M.B. LigPlot+: multiple ligand-protein interaction diagrams for drug discovery. *J Chem Inf Model* **51**, 2778-2786 (2011).